

## ARTICLE

# Effect of Molybdenum Doping on Oxygen Permeation Properties and Chemical Stability of $\text{SrCo}_{0.8}\text{Fe}_{0.2}\text{O}_{3-\delta}$

Chun-lin Song<sup>a\*</sup>, Shu-min Fang<sup>b\*</sup>*a. Faculty of Materials and Energy, Southwest University, Chongqing 400715, China**b. Department of Mechanical Engineering, University of South Carolina, Columbia, SC 29208, USA*

(Dated: Received on March 16, 2014; Accepted on June 16, 2014)

The phase composition, microstructure, thermal expansion coefficients, oxygen permeation properties and chemical stability of  $\text{SrCo}_{0.7}\text{Fe}_{0.2}\text{Mo}_{0.1}\text{O}_{3-\delta}$  (SCFM) were investigated and compared with those of  $\text{SrCo}_{0.8}\text{Fe}_{0.2}\text{O}_{3-\delta}$  (SCF). Single phase SCFM was successfully prepared by a combined EDTA-citric method. SCFM shows a lower thermal expansion coefficient ( $24 \times 10^{-6} - 29 \times 10^{-6} / \text{K}$ ) than SCF between 500 and 1050 °C, indicating a more stable structure. SCFM shows a high oxygen permeation flux, although the oxygen flux of SCFM decreases slightly because of Mo dopant. Furthermore, it was demonstrated that the doping of Mo in SCF can prevent the order-disorder transition and improves the chemical stability to  $\text{CO}_2$ .

**Key words:** Oxygen permeation,  $\text{SrCo}_{0.8}\text{Fe}_{0.2}\text{O}_{3-\delta}$ , Chemical stability, Molybdenum

## I. INTRODUCTION

The vast combustion of fossil fuels results in an enormous emission of  $\text{CO}_2$ , which is believed to be one of the key factors for global warming. Thus, it draws a lot of attention to the development of an efficient combustion process incorporated with  $\text{CO}_2$  capture and sequestration (CCS) [1]. Recently, a system, in which pure oxygen was supplied to the burner, was proposed. The burner released a flue gas only consisting of  $\text{CO}_2$  and water to avoid costs in the step of separating  $\text{N}_2$  from  $\text{CO}_2$  before the sequestration of  $\text{CO}_2$  [2]. However, present technologies such as cryogenic distillation are quite expensive for producing pure oxygen. A membrane reactor, in which only oxygen is supplied to fossil fuels, is a promising way. Dense mixed oxygen ion/electron conductors (MIECs), showing 100% oxygen selectivity, are the most promising materials for this application. Except high oxygen permeation property, the most important challenges are the mechanical and chemical stability of MIECs, especially in a  $\text{CO}_2$  atmosphere [3–6].

Among the types of MIECs, cobalt-based perovskite oxides with composition of  $(\text{Ln,A})(\text{Co,B})\text{O}_{3-\delta}$  (Ln=rare earth elements, A=Ca, Sr, and Ba, B=transition metal elements) show the highest oxygen ionic conductivity, making them one of the promising oxygen separation materials. Although Ba-containing

perovskite oxides show a very high oxygen permeation flux, their chemical stability is too low in  $\text{CO}_2$  [7–9]. As one of the most promising MIECs,  $\text{SrCo}_{0.8}\text{Fe}_{0.2}\text{O}_{3-\delta}$  (SCF) shows not only higher oxygen permeation flux, but also better chemical stability in  $\text{CO}_2$  than that of Ba-based perovskite [4, 10–15]. However, its chemical stability still needs to be improved in order to withstand the cruel conditions in oxy-fuel process. Furthermore, SCF shows a high thermal expansion coefficient (TEC) [16, 17], which needs to be reduced for the match with sealing materials.

Recently, substitution with high valence cations (*e.g.*, Ti, Zr, Nb, Ta) has been found to decrease TEC and improve the structural and chemical stability in  $\text{CO}_2$  [4, 6, 7, 18]. With a higher valence than Ti, Zr, Nb, and Ta,  $\text{Mo}^{6+}$  may be more effective to improve the chemical stability of SCF in  $\text{CO}_2$ . The ionic radius of  $\text{Mo}^{6+}$  (0.59 Å) is close to that of  $\text{Co}^{4+}$  and  $\text{Co}^{3+}$  (0.53 and 0.61 Å, respectively) [19], which ensures a high solubility in the perovskite structure of SCF. Actually, Mo-doping in  $\text{Sr}_{0.7}\text{Ba}_{0.3}\text{FeO}_{3-\delta}$  significantly improves its chemical stability in  $\text{CO}_2$  [20]. However, up to date, the effect of Mo doping on these properties of SCF has not been reported.

In this work, we investigated the phase composition, microstructure, thermal expansion coefficient, oxygen permeation properties, and chemical stability of  $\text{SrCo}_{0.7}\text{Fe}_{0.2}\text{Mo}_{0.1}\text{O}_{3-\delta}$ . The role of Mo-doping was also illustrated.

\*Authors to whom correspondence should be addressed. E-mail: shuming@cec.sc.edu, chunlinsong@swu.edu.cn, Tel.: +1-803-7770007, +86-18883327083

## II. EXPERIMENTS

$\text{SrCo}_{0.7}\text{Fe}_{0.2}\text{Mo}_{0.1}\text{O}_{3-\delta}$  (SCFM) powder was prepared by a combined ethylenediaminetetraacetic acid (EDTA)-citric acid method. Stoichiometric amounts of  $\text{Sr}(\text{NO}_3)_2$ ,  $\text{Co}(\text{NO}_3)_2 \cdot 6\text{H}_2\text{O}$ ,  $\text{Fe}(\text{NO}_3)_3 \cdot 9\text{H}_2\text{O}$ , and  $\text{MoO}_3$  (Sigma-Aldrich, >99%) were first dissolved in distilled water or dilute nitric acid under heating and stirring. EDTA (dissolved in ammonia) and citric acid were added as complexation agents, with the molar ratio of EDTA/citric acid/total metal cations set at 1:1.5:1. The pH value of the solution was adjusted by ammonia to  $\sim 7$ . Appropriate amount of ammonium nitrate was then added as a trigger for combustion. Then the solution was heated at 120–150 °C under stirring to evaporate water until it changed into a viscous gel. The viscous gel was heated to form a lot of foam, and finally vigorous combustion took place, resulting in fluffy powder. The powder was then calcined at 950 °C for 5 h to obtain single phase SCFM powder.

SCFM powder was uniaxially pressed at 50 MPa to disk membranes, followed by isostatic pressing at 400 MPa for 3 min. The obtained membranes were sintered at 1230 °C for 5 h at a heating and cooling rate of 2 °C/min. The phase composition of powder and sintered membranes was characterized by X-ray diffraction (XRD, Philips X'pert). The microstructure was investigated by scanning electron microscope (SEM, JEOL JSM-5600LV). The density was measured by the Archimedes method in mercury. Thermal expansion behavior was measured using dilatometer (Netzsch Dil-402C) in static air from 20 °C to 1050 °C at a heating rate of 3 °C/min. To investigate the chemical stability of SCFM in  $\text{CO}_2$ -containing atmosphere, the weight gain of SCFM powder was tested in 71% $\text{CO}_2/\text{N}_2$  at 900 °C.

Both surfaces of sintered membranes were polished with silicon carbide sandpapers (120, 320, 600 grits) before the oxygen permeation measurement. All the membranes were polished to 1 mm thickness. The oxygen permeation performance was measured in a quartz reactor with glass ring (Schott 8252) sealed at 1000 °C for 60 min. The oxygen permeation performance was measured from 800 °C to 900 °C with an interval of 25 °C in a quartz reactor sealed with a glass ring at 1000 °C for 1 h. The feed gas was 100 mL/min synthetic air, and the sweep gas was 30 mL/min He. In order to test the performance in  $\text{CO}_2$ , the sweep gas was switched into a mixture of He and  $\text{CO}_2$  to obtain 6%, 8%, 10%, and 100% $\text{CO}_2/\text{He}$ . The composition of the exhaust from sweep side was analyzed by a gas chromatograph (GC, Varian CP-4900) equipped with packed column (filled with 5 Å molecular sieve) and thermal conductivity detector using He as carrier gas. The flow rate of the exhaust gas from the sweep side was measured by a digital flow meter (Varian ADM1000). The leakage through incomplete sealing was checked by measuring  $\text{N}_2$  concentration in the sweep gas. The de-

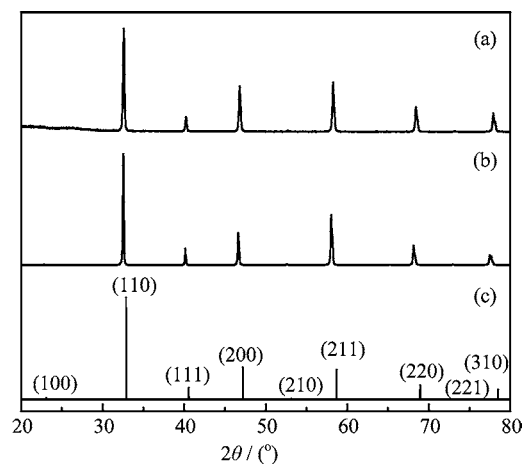


FIG. 1 XRD patterns of different sample. (a) SCFM powder calcined at 950 °C for 10 h, (b) SCFM membrane sintered at 1230 °C for 5 h, and (c) standard pattern of  $\text{SrCo}_{0.81}\text{Fe}_{0.19}\text{O}_{2.78}$  (JCPDS No.82-2445).

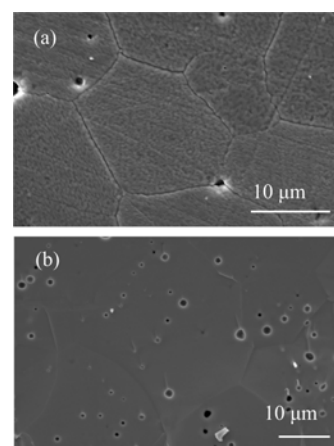


FIG. 2 SEM images of sintered SCFM membrane. (a) Surface and (b) cross-section.

tected leakage was less than 2% in all cases, suggesting that an effective sealing was obtained.

## III. RESULTS AND DISCUSSION

Figure 1 shows the XRD patterns of calcined SCFM powder and sintered SCFM membrane. After calcination at 950 °C for 10 h, a pure perovskite phase has been formed, confirming the high solubility of Mo in SCF. All the diffraction lines can be well indexed, referring to standard pattern of  $\text{SrCo}_{0.81}\text{Fe}_{0.19}\text{O}_{2.78}$  (JCPDS No.82-2445). The result suggests that the fabricated SCFM possesses perovskite structure. The calculated lattice parameter is 3.889 Å, slightly larger than 3.871 Å of SCF [21], which is consistent with the fact that  $\text{Mo}^{6+}$  is larger than  $\text{Co}^{4+}$  (0.59 and 0.53 Å, respectively) [19].

Figure 2 shows the surface and cross-section SEM

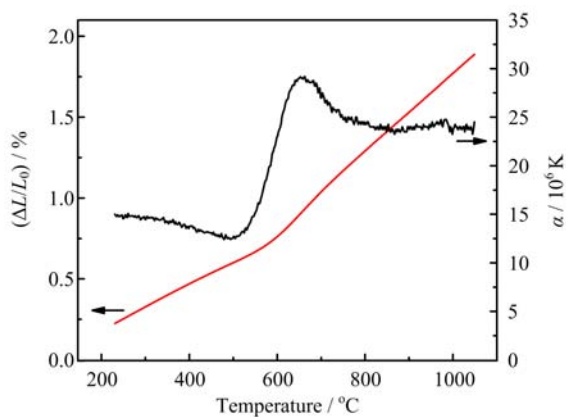


FIG. 3 Thermal expansion behavior of SCFM.

images of SCFM membrane sintered at 1230 °C for 5 h. The membrane is dense with grain size of 10–20  $\mu\text{m}$ . Some small pores were also observed both on the surface and the section. In agreement with the dense microstructure, the relative density measured by Archimedes method is 93.9%. Although these micro pores exist, the sample is still gas-tight, enabling oxygen permeation measurement.

Figure 3 shows the thermal expansion behavior of SCFM measured in static air by dilatometry. Due to the release of oxygen from the oxide at elevated temperatures, two regions were observed. At the low temperatures (200–500 °C), the TEC ( $\alpha$ ) varies between  $12.5 \times 10^{-6}$  and  $15.0 \times 10^{-6}/\text{K}$ . At the high temperatures (500–1050 °C), the TEC first quickly increases to  $29.0 \times 10^{-6}/\text{K}$  and then decreases to  $\sim 24.0 \times 10^{-6}/\text{K}$ . The sudden increase in TEC is due to the reduction of  $\text{Co}^{4+}$  and  $\text{Fe}^{4+}$  to  $\text{Co}^{3+}$  and  $\text{Fe}^{3+}$ , respectively [22]. The ionic radii of low valence cations is larger than that of high valence ones. The reduction process is also coupled with loss of oxygen and formation of additional oxygen vacancies in SCFM lattice. Both the reduction of high valence cations and formation of oxygen vacancies can cause expansion of lattice, which is called chemical expansion [23]. The reported TEC of SCF ( $39 \times 10^{-6}/\text{K}$  [16],  $34 \times 10^{-6} - 29 \times 10^{-6}/\text{K}$  [21]) are significantly higher than that of SCFM, suggesting Mo-doping reduces the TEC of SCF. It is beneficial for the resistance of the membranes to heating/cooling cycles.

Figure 4 shows the Arrhenius plots of oxygen permeation flux  $J_{\text{O}_2}$  through SCFM membrane. An order-disorder transition of oxygen vacancies was reported in SCF at  $\sim 790$  °C first by Kruidhof *et al.* [24]. Later, the transition temperature was reported to be  $\sim 810$  °C [16, 17, 25]. It was reported that the doping of Sc, Y, Al, Ti, Zr, Nb, and Ta at Co-sites could stabilize the perovskite structure of SCF, and the order-disorder transition was suppressed or prevented [4, 14, 17, 26–29]. Figure 4 shows no significant bending in the range of 800–825 °C, indicating that the order-

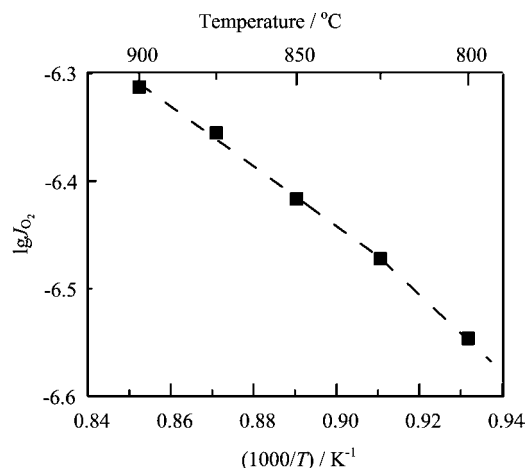


FIG. 4 Arrhenius plot of oxygen permeation flux through SCFM membrane under air/He gradient. Membrane thickness=1.0 mm.

disorder transition is suppressed or prevented to a large extent. The results suggest that Mo-doping plays an important role in stabilizing the perovskite structure of SCF. The activation energy of SCFM between 800 and 900 °C is  $53.2 \pm 2.1$  kJ/mol, which is slightly higher than that of SCF ( $\sim 46$  kJ/mol) [25]. Similar increase in activation energy is also observed in Zr and Nb-doped SCF [14, 17]. The flux of SCFM at 800 and 900 °C is 0.28 and 0.48  $\mu\text{mol}/\text{cm}^2\text{s}$ , respectively, which is slightly lower than that of SCF (0.48 and 0.76  $\mu\text{mol}/\text{cm}^2\text{s}$ , respectively) [25]. However, the oxygen permeation flux is comparable with that of 5wt% $\text{Nb}_2\text{O}_5$ -doped  $\text{SrCo}_{0.8}\text{Fe}_{0.2}\text{O}_{3-\delta}$  (0.27 and 0.48  $\mu\text{mol}/\text{cm}^2\text{s}$ , respectively) [17]. Compared with SCF, the decreased oxygen permeation flux may come from the change in microstructure and phase composition. Firstly, the grain size of SCFM is rather big (10–20  $\mu\text{m}$ ), which is detrimental for oxygen permeation. For example, Zhang *et al.* reported the flux of SCF with average grain size of 14.8  $\mu\text{m}$  is only  $\sim 66\%$  of that at 900 °C (4.1  $\mu\text{m}$ ), which is attributed to the higher oxygen ionic conductivity in grain boundaries than inside grain [11]. Therefore, it can be anticipated that the oxygen permeation flux through SCFM membrane can be improved by obtaining a smaller grain size. Secondly, the doping of high valence cations at Co sites is expected to decrease the concentration of oxygen vacancies, and the strong Mo-O also contributes the difficulty for oxygen diffusion, therefore, the activation energy for oxygen permeation increases and the oxygen permeation flux decreases.

Figure 5 shows the weight quickly increases after the exposure to  $\text{CO}_2$  and finally is stabilized with a weight gain of  $\sim 9\%$ . It is rather low compared with the theoretical weight gain of 22% when SCF is totally transformed into strontium carbonate and cobalt and iron oxides. Here, it is worth mentioning that the constant metal valence and no oxygen release from

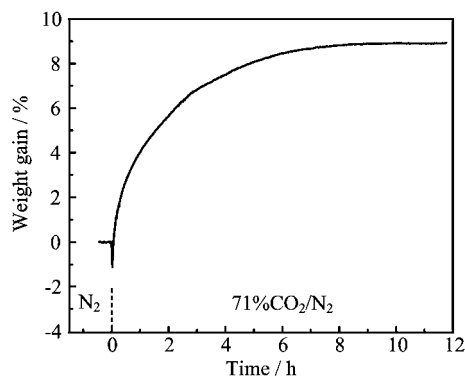


FIG. 5 Weight change of SCFM powder upon exposure to 71% CO<sub>2</sub> at 900 °C.

SrCo<sub>0.7</sub>Fe<sub>0.2</sub>Mo<sub>0.1</sub>O<sub>3-δ</sub> are assumed at the atmosphere of CO<sub>2</sub>. The result implies that the crystal structure of SCFM is more stable than that of SCF, and the reaction between CO<sub>2</sub> and SCFM may be limited on the surface, rather than inside the bulk. Similarly, the weight gain of SCF and SrCo<sub>0.72</sub>Fe<sub>0.18</sub>Ti<sub>0.1</sub>O<sub>3-δ</sub> measured by similar method is ~19% and 8% at 950 °C, respectively. Therefore, the doping of Mo can improve the chemical stability of SCF in CO<sub>2</sub>.

For further investigation, the performance of oxygen permeation of SCFM in CO<sub>2</sub> was also studied. Figure 6 shows the oxygen permeation flux through SCFM membrane in different concentration of CO<sub>2</sub>. The oxygen permeation flux through SCFM membrane was 0.87 μmol/cm<sup>2</sup>s under air/He gradient, and decreased to 0.82, 0.67, 0.46 and 0.21 μmol/cm<sup>2</sup>s, when sweep gas was switched to 6%, 8%, 10%, 100%CO<sub>2</sub>/N<sub>2</sub>, respectively. The degradation was fast and quickly reached equilibrium within 5 h. It was reported that the oxygen permeation flux through SCF membrane continuously decreased from 1.26 μmol/cm<sup>2</sup>s to 0.18 μmol/cm<sup>2</sup>s in 75 h after sweep gas was switched from He to 100% CO<sub>2</sub> [4], and the flux through SCF membrane didn't reach a stable stage, so the flux was expected to degrade more if the measurement was continued. Thus, the chemical stability to CO<sub>2</sub> of SCFM is better than that of SCF. The enhanced chemical stability of SCFM is attributed to the higher bonding energy of Mo–O (607.3 kJ/mol) than that of Co–O (384.5 kJ/mol), leading to a lower tendency for O<sup>2-</sup> to donate electrons to charged carbon atom. It is worthy to mention that the oxygen permeation flux is totally recovered quickly when CO<sub>2</sub> is removed from the sweep gas (Fig.6), this phenomenon agrees with the results of weight change of SCFM powder upon exposure to CO<sub>2</sub> (Fig.5), indicating that Mo-doping successfully stabilizes the perovskite structure of SCF and improves its chemical stability to CO<sub>2</sub>.

#### IV. CONCLUSION

The phase composition, microstructure, oxygen permeation properties, and chemical stability of

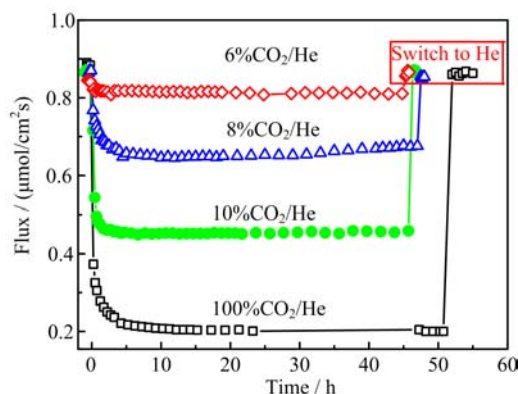


FIG. 6 Time dependence of oxygen permeation flux through SCFM membrane in a sweep gas containing different content of CO<sub>2</sub>. It is also shown that the permeation flux is totally recovered quickly when CO<sub>2</sub> is removed from the sweep gas.

SrCo<sub>0.7</sub>Fe<sub>0.2</sub>Mo<sub>0.1</sub>O<sub>3</sub> (SCFM) are compared with those of SrCo<sub>0.8</sub>Fe<sub>0.2</sub>O<sub>3</sub> (SCF). Phase-pure SCFM was successfully prepared via a combined EDTA-citric method. Dense SCFM membrane was obtained with grain size 10–20 μm. SCFM membrane shows a lower thermal expansion coefficient than that of SCF, indicating a more stable crystal structure than that of SCF. Because of the higher bonding energy of Mo–O, the oxygen permeation flux of SCFM is slightly decreased, on the other hand, the chemical stability of SCFM is improved to a large extent.

#### V. ACKNOWLEDGMENTS

This work was supported by the Fundamental Research Funds for the Central Universities (No.SWU113045 and No.XDJK2013C089).

- [1] J. Davison, *Energy* **32**, 1163 (2007).
- [2] M. Balaguer, J. Garcia-Fayos, C. Solis, and J. M. Serra, *Chem. Mater.* **25**, 4986 (2013).
- [3] X. Y. Tan, K. Li, A. Thursfield, and I. S. Metcalfe, *Catal. Today* **131**, 292 (2008).
- [4] Q. Zeng, Y. B. Zuo, C. G. Fan, and C. S. Chen, *J. Membr. Sci.* **335**, 140 (2009).
- [5] S. Fang, C. Chen, and L. Winnubst, *Solid State Ionics* **190**, 46 (2011).
- [6] J. Yi, M. Schroeder, and M. Martin, *Chem. Mater.* **25**, 815 (2013).
- [7] J. Yi, M. Schroeder, T. Weirich, and J. Mayer, *Chem. Mater.* **22**, 6246 (2010).
- [8] M. Schulz, R. Kriegel, and A. Kämpfer, *J. Membr. Sci.* **378**, 10 (2011).
- [9] M. Arnold, H. H. Wang, and A. Feldhoff, *J. Membr. Sci.* **293**, 44 (2007).
- [10] Y. Teraoka, H. M. Zhang, S. Furukawa, and N. Yamazoe, *Chem. Lett.* 1743 (1985).

- [11] K. Zhang, Y. L. Yang, D. Ponnusamy, A. J. Jacobson, and K. Salama, *J. Mater. Sci.* **34**, 1367 (1999).
- [12] Z. T. Wu, W. Q. Jin, and N. P. Xu, *J. Membr. Sci.* **279**, 320 (2006).
- [13] J. X. Yi, S. J. Feng, Y. B. Zuo, W. Liu, and C. S. Chen, *Chem. Mater.* **17**, 5856 (2005).
- [14] W. Chen, Y. B. Zuo, C. S. Chen, and A. J. A. Winubst, *Solid State Ionics* **181**, 971 (2010).
- [15] J. L. Li, Q. Zeng, T. Liu, and C. S. Chen, *Sep. Purif. Technol.* **77**, 76 (2011).
- [16] C. G. Fan, Z. Q. Deng, Y. B. Zuo, W. Liu, and C. S. Chen, *Solid State Ionics* **166**, 339 (2004).
- [17] G. Zhang, Z. Liu, N. Zhu, W. Jiang, X. Dong, and W. Jin, *J. Membr. Sci.* **405-406**, 300 (2012).
- [18] H. Zhao, D. Teng, X. Zhang, C. Zhang, and X. Li, *J. Power Sources* **186**, 305 (2009).
- [19] R. D. Shannon, *Acta Crystallogr. A* **32**, 751 (1976).
- [20] X. Dong, W. Jin, and N. Xu, *Chem. Mater.* **22**, 3610 (2010).
- [21] O. Y. Podyacheva, Z. R. Ismagilov, A. N. Shmakov, M.G. Ivanov, A. N. Nadeev, S. V. Tsybulya, and V. A. Rogov, *Catal. Today* **147**, 270 (2009).
- [22] S. McIntosh, J. F. Vente, W. G. Haije, D. H. A. Blank, and H. J. M. Bouwmeester, *Solid State Ionics* **177**, 1737 (2006).
- [23] S. McIntosh, J. F. Vente, W. G. Haije, D. H. A. Blank, and H. J. M. Bouwmeester, *Chem. Mater.* **18**, 2187 (2006).
- [24] H. Kruidhof, H. J. M. Bouwmeester, R. H. E. Vondoor, and A. J. Burggraaf, *Solid State Ionics* **63-65**, 816 (1993).
- [25] Z. P. Shao, G. X. Xiong, J. H. Tong, H. Dong, and W. S. Yang, *Sep. Purif. Technol.* **25**, 419 (2001).
- [26] X. L. Dong, Z. Xu, X. F. Chang, C. Zhang, and W. Q. Jin, *J. Am. Ceram. Soc.* **90**, 3923 (2007).
- [27] T. Nagai, W. Ito, and T. Sakon, *Solid State Ionics* **177**, 3433 (2007).
- [28] P. Y. Zeng, Z. P. Shao, S. M. Liu, and Z. P. Xu, *Sep. Purif. Technol.* **67**, 304 (2009).
- [29] K. Zhang, R. Ran, Z. Shao, Z. Zhu, Y. Jin, and S. Liu, *Ceram. Int.* **36**, 635 (2010).